Supporting Information

Van Damme et al. 10.1073/pnas.1017890108

SI Materials and Methods

Cloning of Constructs. TPLATE-GFP, FH5-GFP, GFP-MBD, RFP-TUA2, GFP-AIR9, and GFP-KCA1 were described elsewhere (1–6). The *Agrobacterium* strain containing 35S::mVENUS-PH_{FAPP1} (7) was a kind gift from Joop Vermeer (University of Lausanne, Lausanne, Switzerland). pH7RWG2-TPLATE was constructed by a single gateway (Invitrogen) reaction using pDONR207-TPLATE (1) and pH7RWG2 (8). Entry clones of clathrin light chain 2 (CLC2) (At2g40060) with and without stop codon (9) were used in single Gateway reactions to construct the pK7FWG2-CLC2 (Fig. S8 and Movie S2) and pK7WGF2-CLC2 (Fig. 2) expression clones. The entry clone of CLC2 without stop codon was used in a triple Gateway reaction, together with pDONRP4-P1R-P35S, pDONRP2-P3R-mCHERRY, and pH7m34GW (8) to yield pH7m34GW-P35S::CLC2-mCHERRY (Fig. 1, Fig. S2, and Movie S3).

Bimolecular fluorescence complementation (BiFC) constructs for 35S::ORF-TAG using the N- and C-terminal halves of EGFP were constructed by triple Gateway reactions using pK7m34GW or pH7m34GW (8) as described (10) using pDONR207 and pDONR221 entry clones of TPLATE, CLC2, and CHC1 (At3g08530) without stop codon. *Arabidopsis* CHC1 without stop codon was amplified using the following primer pairs: B1F-CHC1—5′ *GGGGACAAGTTTGTACAAAAAAGCAGCT*CCA-CCATGGCGGCTGCCAACGCCC 3′; and B1R-CHC1nostop—5′ *GGGGACCACTTTGTACAAGAAAGCTGGGTC*GTAGCC-GCCCATCGGTGGCATTC 3′).

35S::TAG-ORF clones were constructed by double Gateway recombination using a modified pH7m24GW destination vector with a 35S promotor incorporated before the attB4B2 cassette (10). The N-terminal fragment of EGFP in pDONRP4P1R was combined with pDONR207 or pDONR221 entry clones containing TPLATE, CLC2, and CHC1 with stop codon. The N-terminal fragment of EGFP was amplified using the following primers: B4F-headEGFP—5′ *GGGGACAACTTTGTATAGAAAAGTTGGG*-ATGGTGAGCAAGGGCGAGGAGCTGTTCA 3′; and B1R-headEGFP—5′ *GGGGACTGCTTTTTTGTACA AACTTGT*GG-CCATGATATAGACGTTGTGGCTGTTGTA 3′) and combined by Gateway reaction into pDONRP4P1R. The TPLATE and CHC1 ORFs with stop codon were amplified using the following primer pairs: B1F-TPLATE—5′ *GGGGACAAGTTTGTACAAAA-AAGCAGGCT*ATGGACATTC TTTTTGCTCAGATCC 3′; B2R-TPLATEstop—5′ *GGGGACCACTTTGTACAAGAAAGCTGGG-T*TTAGTTAA CTTTGGTATATTTTCTATCTTTGCA 3′; B1F-CHC1—5′ *GGGGACAAGTTTGTACAAAAAAGCAGCT*CCAC CATGGCGGCTGCCAACGCCC 3′; and B2R-CHC1stop—5′ *GG-GGACCACTTTGTACAAGAAAGCTGGGT*CTTA GAGCCGCC-CATCGGTGGCATTC 3′).

BY-2 Transformation. Stable BY-2 transformation was carried out as described by Geelen and Inzé (11). BY-2 cell lines expressing two fluorescent constructs were created by consecutive super-transformation of single transformed lines. Stably transformed calli were screened for fluorescence, and localization patterns of tagged proteins were confirmed by analyzing several independent transformants.

***Arabidopsis* Lines.** The *Arabidopsis* line expressing 35S::CLC2-EGFP was described elsewhere (12). *Arabidopsis* plants expressing a genomic construct of TPLATE fused to GFP (13) were crossed with homozygous *gnl1-1* plants (14) and heterozygous *cpi1-1* plants (15). After selfing, homozygous *gnl1-1* mutants expressing genomic TPLATE-GFP were identified by growing the lines on 1/2 strength Murashige and Skoog (MS) medium supplemented with 25 μM Brefeldin A (BFA) and by subsequent screening of the *gnl-1–1* mutants for GFP fluorescence. Homozygous *cpi1-1* seedlings expressing TPLATE-GFP were phenotypically identified on 1/2 MS medium by a one-in-four segregation of the offspring seeds and by subsequent screening for GFP fluorescence.

Transient Expression of BiFC Constructs. Wild-type *Nicotiana benthamiana* plants (3–4 wk old) were used to transiently express the various BiFC construct combinations by *Agrobacterium tumefaciens* (strain LBA4404)-mediated transient transformation of lower epidermal leaf cells as previously described (10) using a modified buffer [10 mM $MgCl_2$ (1 M stock solution; Merck); 10 mM 2-(N-morpholino)ethanesulfonic acid (MES) (0.5 M stock solution; Duchefa); 100 μM Acetosyringone (100 mM stock solution; Sigma Aldrich)] and addition of a P19-expressing *Agrobacterium* strain to boost protein expression (16). All *Agrobacterium* strains were grown for 2 d, diluted to OD 0.5 in infiltration buffer, and incubated for 2 h at room temperature before mixing in a 1:1 ratio with other strains and injecting. After 3–5 d of incubation, interaction of the proteins was scored by screening lower epidermal cells for fluorescence using confocal microscopy.

Chemical Treatments. Stock solutions were prepared of BFA (50 mM in DMSO, 1000–2000× stock; Molecular Probes), propyzamide (6 mM in DMSO, 1000× stock; Chem Service Inc.), caffeine (500 mM in water, 100× stock; Sigma Aldrich), Concanamycin A (2 mM in DMSO, 1000× stock; Sigma Aldrich), aniline blue (0.5% in water; Sigma Aldrich), Latrunculin B (20 mM in DMSO, 1000× stock; Sigma Aldrich), Tyrphostin A23 and A51 (50 mM in DMSO, 1000–500× stock; Sigma Aldrich), Wortmannin (20 mM in DMSO, 666× stock; Sigma Aldrich), and FM4-64 (2 mM in water, 500–250× stock; Molecular Probes). Caffeine, BFA, and Concanamycin A treatments of *Arabidopsis* seedlings were performed by incubating the seedlings in liquid 1/2 strength MS medium supplemented with 5 mM caffeine, 50 μM BFA, or 2 μM Concanamycin A for 2 h in the light under slight agitation. Seedlings were subsequently incubated with 8 μM FM4-64 before imaging. Tyrphostin treatments were carried out in liquid 1/2 strength MS for 30 min in the dark at room temperature, followed by a 10-min incubation with FM4-64 (4 μM). Wortmannin treatments were performed by incubating seedlings in 1/2 strength MS supplied with 30 μM Wortmannin in the presence of 2 μM FM4-64 for 1 h in the dark at room temperature.

Confocal Microscopy. Image acquisition was obtained with a 100M inverted confocal microscope (Zeiss) with software package LSM510, version 3.2, equipped with a 63× water-corrected objective (n.a. 1.2) using the following settings for EGFP and momomeric red fluorescent protein (mRFP) detection: EGFP excitation at 488 nm; emission filter 500–530 nm; mRFP excitation at 543 nm; and emission using a 560-nm cutoff. Images were also obtained with a FluoView1000 inverted confocal microscope (Olympus) equipped with a water-corrected 60× objective (n.a. 1.2) using 488 nm laser excitation and a spectral detection bandwidth of 500–530 nm for EGFP and 559 nm laser excitation together with a spectral detection bandwidth of 570–670 nm for mCHERRY and FM4-64 detection and with a Zeiss 710 inverted confocal microscope with the ZEN 2009 software

package and equipped with a 40× water corrected objective (n.a. 1.2). GFP was visualized using 488 nm laser excitation and 500–530 nm spectral detection; FM4-64 was visualized using 458 nm laser excitation and 592–754 nm spectral detection. Autofluorescence in the BiFC experiments was visualized using 514 nm laser excitation and 553–703 nm spectral detection. Fluorescence intensity graphs were made using the standard profiling software tools supplied with the LSM510 (Fig. S1) and FluoView1000 (Fig. 1 and Fig. S5) confocal software packages. To reduce the noise in the plots, raw data points were averaged by a 5- or 9-data-point window for Fig. 1 and Fig. S1. For Fig. S5, all images used for quantification were captured using identical confocal settings and sequential channel detection. Reduction in plasma membrane (PM)-associated TPLATE label was visually scored for all individual seedlings by comparing cytoplasmic versus PM-associated signal intensity of cell files captured in the confocal plane. Inhibition of FM4-64 uptake upon Tyrphostin and Wortmannin treatment was scored by the absence of internalized FM4-64 label, detectable under the used confocal conditions, upon increasing the intensity and contrast parameters of the captured images using the FV1000 software.

Arabidopsis seedlings were imaged between slide and cover glass. BY-2 cells were applied to a chambered cover-glass system (Lab-Tek). Cells were immobilized in a thin layer (1 mL) of BY-2 medium containing vitamins (11) and 0.8% low-melting-point agarose (Invitrogen). Chemicals were added to 1 mL of liquid BY-2 medium with added vitamins; drug concentration was adjusted to the final volume of the sample (2 mL) and added to the chambered cover-glass system containing the immobilized cells.

GFP-Based Coimmunoprecipitation and Western Blotting. Total protein extracts were obtained from liquid nitrogen-ground 6-d-old seedlings grown on vertical 1/2 strength Murashige and Skoog (MS) plates using an equal volume (wt/vol) of homogenization buffer [25 mM Tris·HCl, pH 7.6, 5 mM EGTA, 150 mM NaCl, 15 mM *p*-nitrophenylphosphate, 60 mM β-glycerophosphate, 0.1% (vol/vol) Nonidet P-40, 0.1 mM sodium vanadate, 1 mM NaF, 1 mM DTT, 1 mM PMSF, 10 μg/mL leupeptin, 10 μg/mL aprotinin, 5 μg/mL antipain, 5 μg/mL chymostatin, 5 μg/mL pepstatin, 10 μg/mL soybean trypsin inhibitor, 0.1 mM benzamidine, 1 μM transepoxysuccinyl-L-leucylamido-(4-guanidino)butane (E64), 5% (vol/vol) ethylene glycol], which was vortexed thoroughly. Cell debris was centrifuged at 14,000 × *g* for 20 min at 4 °C, and the supernatant was collected as the input fraction. Two milligrams of protein from the input fraction was incubated with 15 μL effective, pre-equilibrated GFP-Trap_A agarose beads (Chromotek) for 1 h, gently rotating at 4 °C. The unbound fraction was removed from the beads after a brief centrifugation at 1,500 × *g* for 1 min at 4 °C. Beads were washed twice with 500 μL homogenization buffer. The bound protein fraction was boiled from the beads with sample buffer at 95 °C for 10 min and loaded onto an 8% SDS/PAGE protein gel, together with 10 μg from the input and unbound fraction. Each gel was loaded in duplicate to detect the GFP-tagged protein and endogenous clathrin heavy chain on different blots. SDS/PAGE separated proteins were blotted on Immobilon-P membranes (Millipore). Membranes were blocked overnight at 4 °C in 3% (vol/vol) milk powder dissolved in 25 mM Tris·HCl, pH 8, 150 mM NaCl, and 0.05% Tween 20. The blots were then incubated at room temperature either with the Living Colors A.v. Monoclonal GFP antibody (1/5,000) (JL-8; Clontech) or the soybean clathrin heavy chain antibody (1/500) (sc-57684; Santa Cruz Biotechnology). Antigen–antibody complexes were detected with anti-mouse horseradish peroxidase-conjugated IgG (1/10,000) (Amersham Biosciences) using chemiluminescence (Perkin-Elmer).

1. Van Damme D, Bouget F-Y, Van Poucke K, Inzé D, Geelen D (2004) Molecular dissection of plant cytokinesis and phragmoplast structure: A survey of GFP-tagged proteins. *Plant J* 40:386–398.
2. Vanstraelen M, et al. (2006) Cell cycle-dependent targeting of a kinesin at the plasma membrane demarcates the division site in plant cells. *Curr Biol* 16:308–314.
3. Ingouff M, et al. (2005) Plant formin AtFH5 is an evolutionarily conserved actin nucleator involved in cytokinesis. *Nat Cell Biol* 7:374–380.
4. Van Damme D, et al. (2004) In vivo dynamics and differential microtubule-binding activities of MAP65 proteins. *Plant Physiol* 136:3956–3967.
5. Buschmann H, et al. (2006) Microtubule-associated AIR9 recognizes the cortical division site at preprophase and cell-plate insertion. *Curr Biol* 16:1938–1943.
6. Marc J, et al. (1998) A GFP-MAP4 reporter gene for visualizing cortical microtubule rearrangements in living epidermal cells. *Plant Cell* 10:1927–1940.
7. Vermeer JEM, et al. (2009) Imaging phosphatidylinositol 4-phosphate dynamics in living plant cells. *Plant J* 57:356–372.
8. Karimi M, De Meyer B, Hilson P (2005) Modular cloning in plant cells. *Trends Plant Sci* 10:103–105.
9. Fujimoto M, Arimura S-i, Nakazono M, Tsutsumi N (2007) Imaging of plant dynamin-related proteins and clathrin around the plasma membrane by variable incidence angle fluorescence microscopy. *Plant Biotechnol* 24:449–455.
10. Boruc J, et al. (2010) Functional modules in the *Arabidopsis* core cell cycle binary protein-protein interaction network. *Plant Cell* 22:1264–1280.
11. Geelen DNV, Inzé DG (2001) A bright future for the Bright Yellow-2 cell culture. *Plant Physiol* 127:1375–1379.
12. Konopka CA, Backues SK, Bednarek SY (2008) Dynamics of *Arabidopsis* dynamin-related protein 1C and a clathrin light chain at the plasma membrane. *Plant Cell* 20:1363–1380.
13. Van Damme D, et al. (2006) Somatic cytokinesis and pollen maturation in *Arabidopsis* depend on TPLATE, which has domains similar to coat proteins. *Plant Cell* 18:3502–3518.
14. Richter S, et al. (2007) Functional diversification of closely related ARF-GEFs in protein secretion and recycling. *Nature* 448:488–492.
15. Men S, et al. (2008) Sterol-dependent endocytosis mediates post-cytokinetic acquisition of PIN2 auxin efflux carrier polarity. *Nat Cell Biol* 10:237–244.
16. Voinnet O, Rivas S, Mestre P, Baulcombe D (2003) An enhanced transient expression system in plants based on suppression of gene silencing by the p19 protein of tomato bushy stunt virus. *Plant J* 33:949–956.

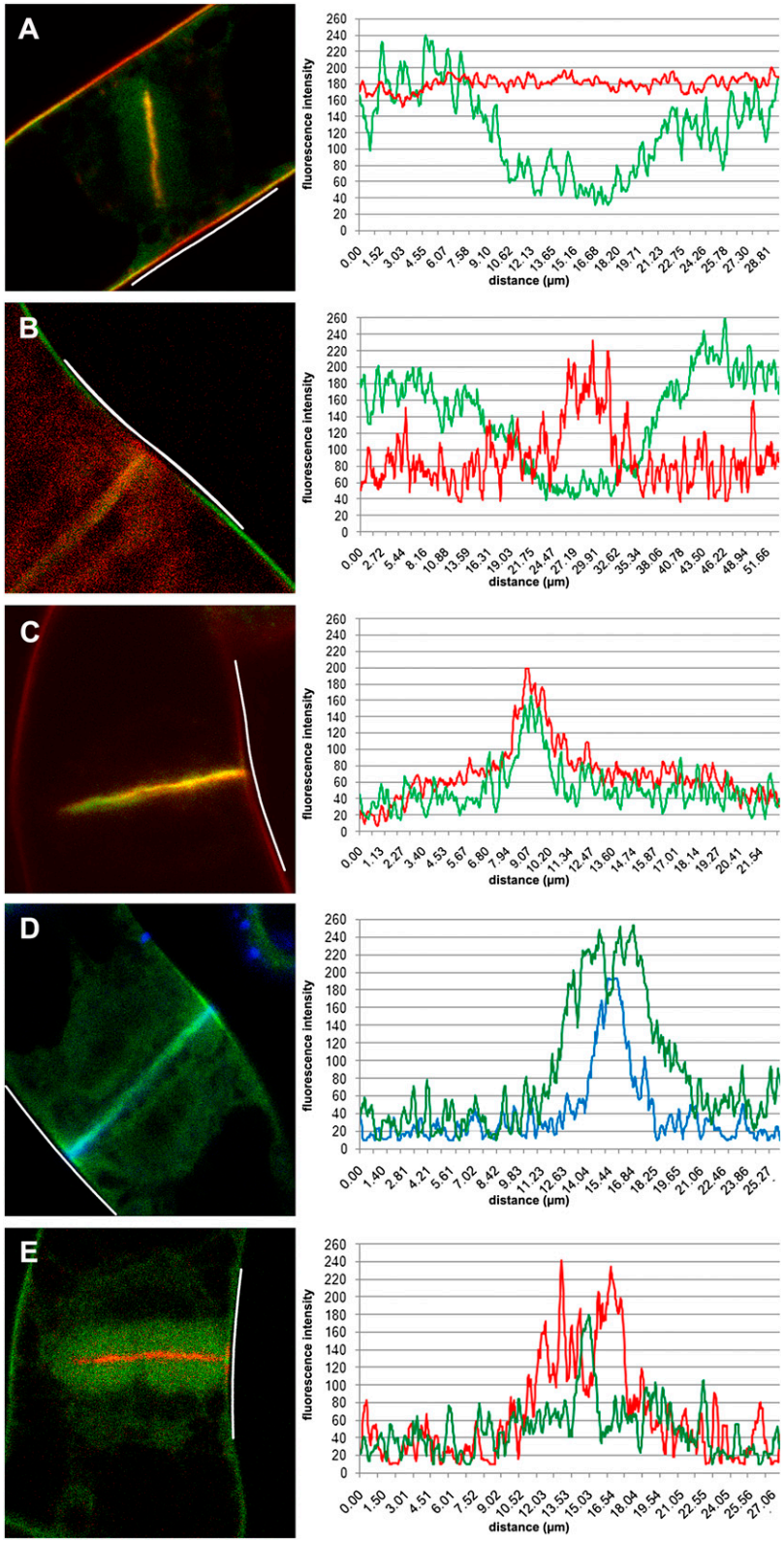

Fig. S1. TPLATE, KCA1, FH5, callose, and AIR9 accumulate differentially at the cortical division zone (CDZ). (*A*) BY-2 cell-expressing GFP-KCA1 (green, *Left*) stained with FM4-64 (red, *Left*) and corresponding fluorescence intensity profiles (GFP-KCA1, green; FM4-64, red, *Right*) spanning the CDZ (white line, *Left*). (*B*) Representative BY-2 cell-expressing GFP-KCA1 (green, *Left*) and TPLATE-RFP (red, *Left*) during cell plate anchoring. The corresponding fluorescence intensity profiles spanning the division zone show the decrease in fluorescence of GFP-KCA1 (green, *Right*) and the accumulation of TPLATE-RFP at the CDZ (red, *Right*). (*C*) BY-2 cell-expressing FH5-GFP (green, *Left*) stained with FM4-64 (red, *Left*) during cell plate anchoring and the corresponding fluorescence intensity profiles showing that the membrane-anchored FH5-GFP (green, *Right*) does not accumulate in the division zone upon anchoring as the width of both fluorescence intensity peaks overlaps. (*D*) BY-2 cell-expressing TPLATE-GFP (green, *Left*) stained with aniline blue (blue, *Left*). Callose, marked by aniline fluorescence, is

Legend continued on following page

restricted to the cell plate insertion site overlapping with the zone of reduced TPLATE accumulation. (*E*) Representative BY-2 cell-coexpressing TPLATE-RFP (red, *Left*) and GFP-AIR9 (green, *Left*). AIR9 accumulates at the cell plate insertion site during anchoring, corresponding to the zone of reduced TPLATE accumulation.

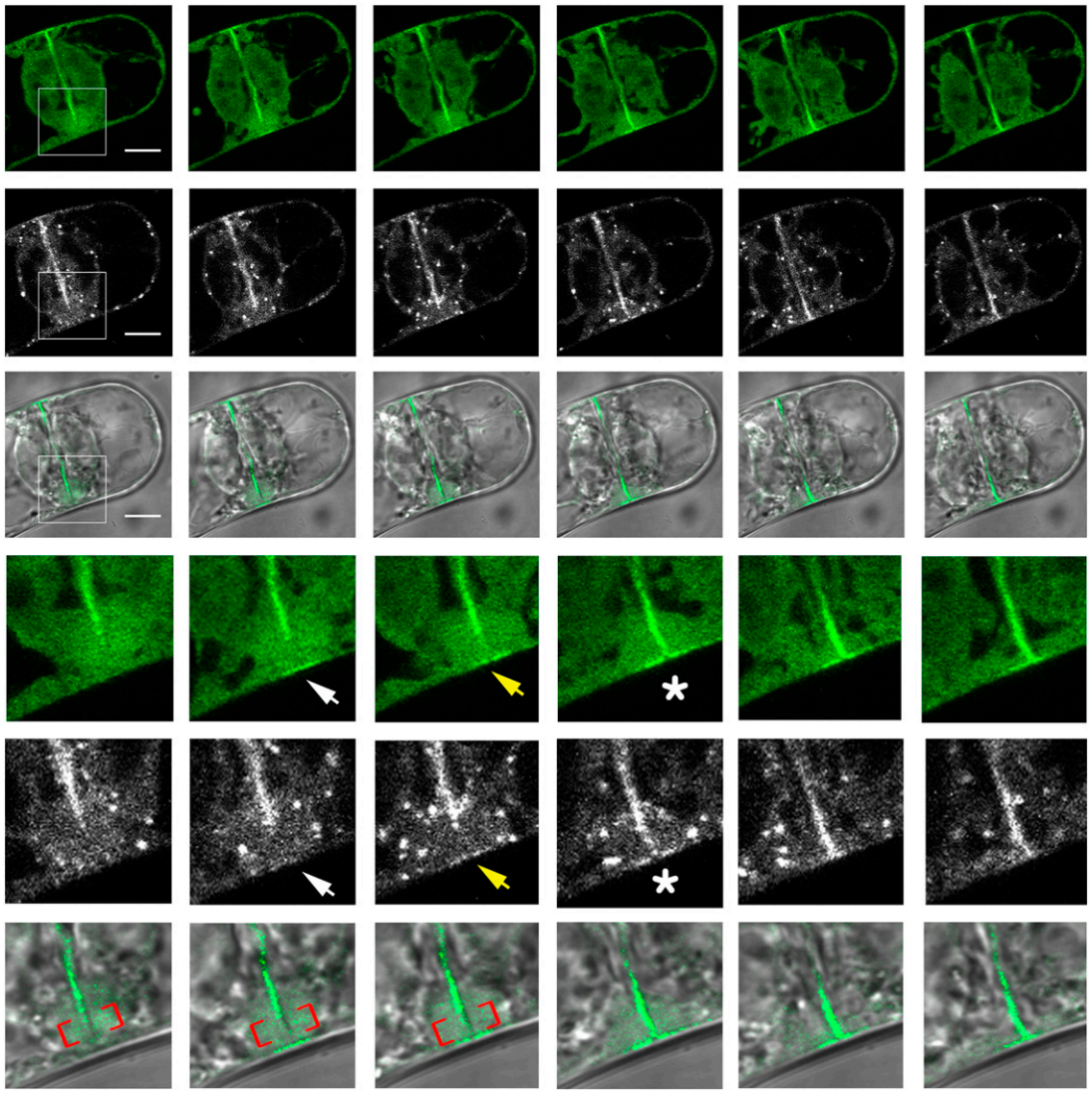

Fig. S2. TPLATE-GFP and CLC2-mCHERRY are specifically targeted to the CDZ. BY-2 cells expressing TPLATE-GFP (first row) and CLC2-mCHERRY (second row) were followed throughout cytokinesis. The third row shows the overlay between TPLATE-GFP and the differential interference contrast (DIC) images. Boxed areas are magnified in the following three rows. TPLATE-GFP accumulates specifically at the division zone without being in contact with the TPLATE-labeled cell plate and accumulates at the CDZ before visible CLC2-mCHERRY signal (white arrows). CLC2-mCHERRY accumulation, unattached from the cell plate, and colocalization with TPLATE-GFP at the division zone is clearly present in the next frame (yellow arrows) and contact between the TPLATE-GFP–labeled part of the cell plate and the CDZ can be observed one frame later (asterisks). The overlay between the DIC image and the TPLATE-GFP signal shows that TPLATE-GFP does not label the outer rim of the plate (red brackets) and that the cell plate fuses with the parental PM before the TPLATE-GFP–labeled cell plate membrane contacts the TPLATE-GFP–labeled CDZ. Represented panels are taken with a 4-min interval. (Scale bars: 10 μm).

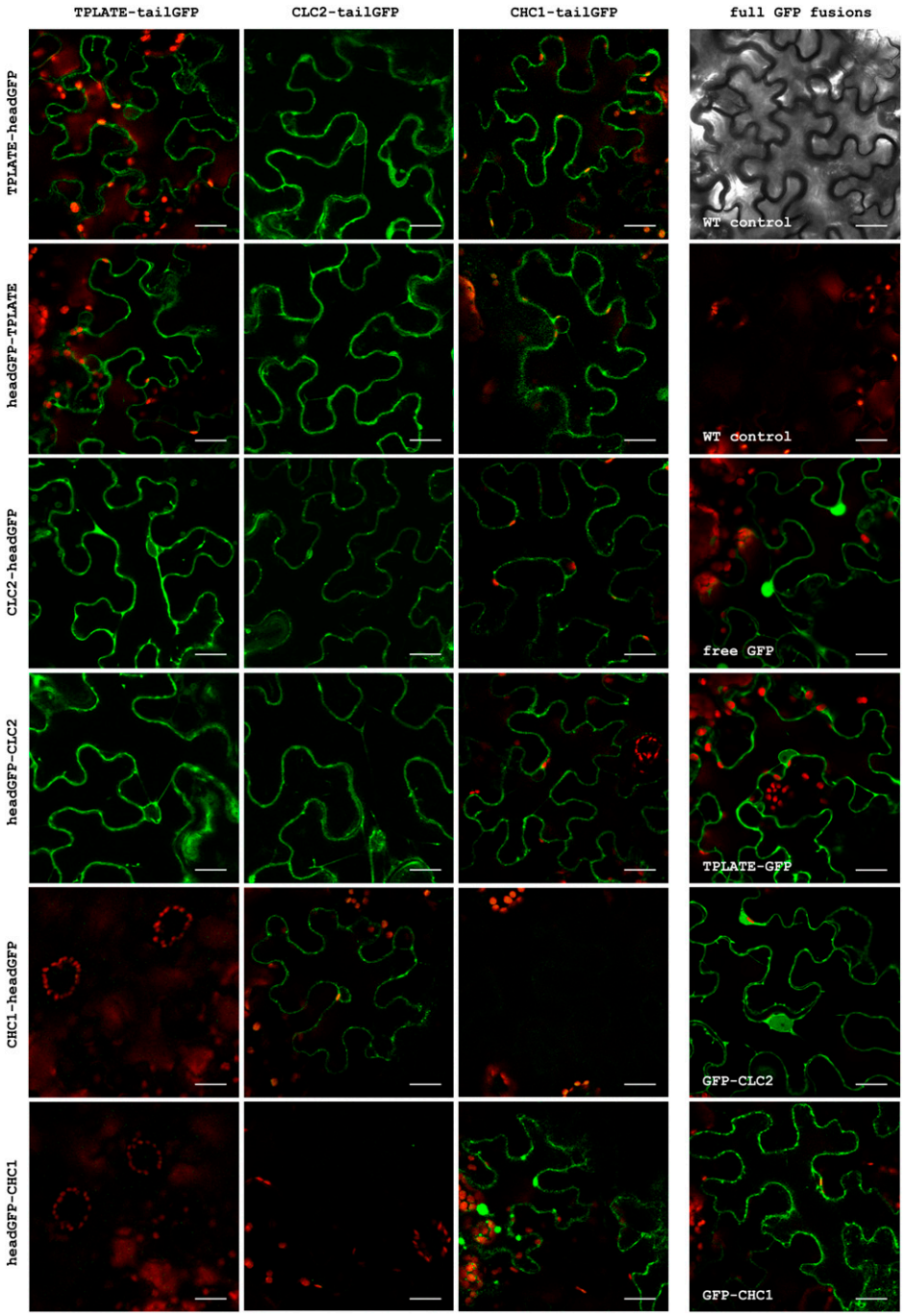

Fig. S3. BiFC interaction between TPLATE, CLC2, and CHC1. Overview of all tested combinations of TPLATE, CLC2, and CHC1 fusion constructs with N- and C-terminal halves of EGFP as shown in Table 1 (N-terminal EGFP: headGFP; C-terminal EGFP: tailGFP). Noninfiltrated leaf (WT control), FreeGFP, and full GFP fusions of TPLATE, CLC2, and CHC1 were used as controls (right column). *Discosoma* sp. red fluorescent protein (DsRed) confocal settings were used to visualize autofluorescence. (Scale bars: 20 μm.)

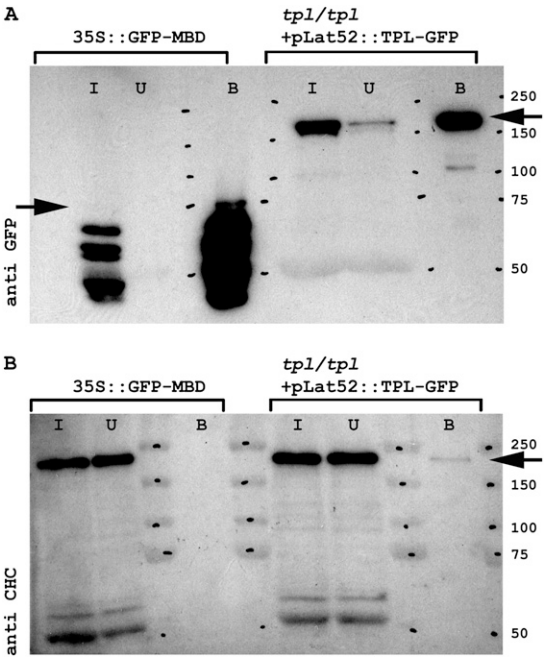

Fig. S4. TPLATE interacts with *Arabidopsis* clathrin heavy chain (CHC) via coimmunoprecipitation. (*A*) Immunoprecipitation and Western blot detection using anti-GFP antibody of GFP-MBD–expressing seedlings (negative control) and seedlings expressing TPLATE-GFP in the *tpl/tpl* mutant background. Both GFP-MBD (81 kDa, arrow) and TPLATE-GFP (160 kDa, arrow) are efficiently enriched in the pellet fraction (B) compared with the input (I) and unbound fraction (U). The GFP-MBD protein is proteolytically degraded during sample preparation, and the full-length fusion is detected only in the pellet fraction. (*B*) Western blot immunodetection of endogenous *Arabidopsis* CHC (193 kDa, arrow) from the fractions in *A*. Endogenous CHC is specifically pulled down by TPLATE-GFP.

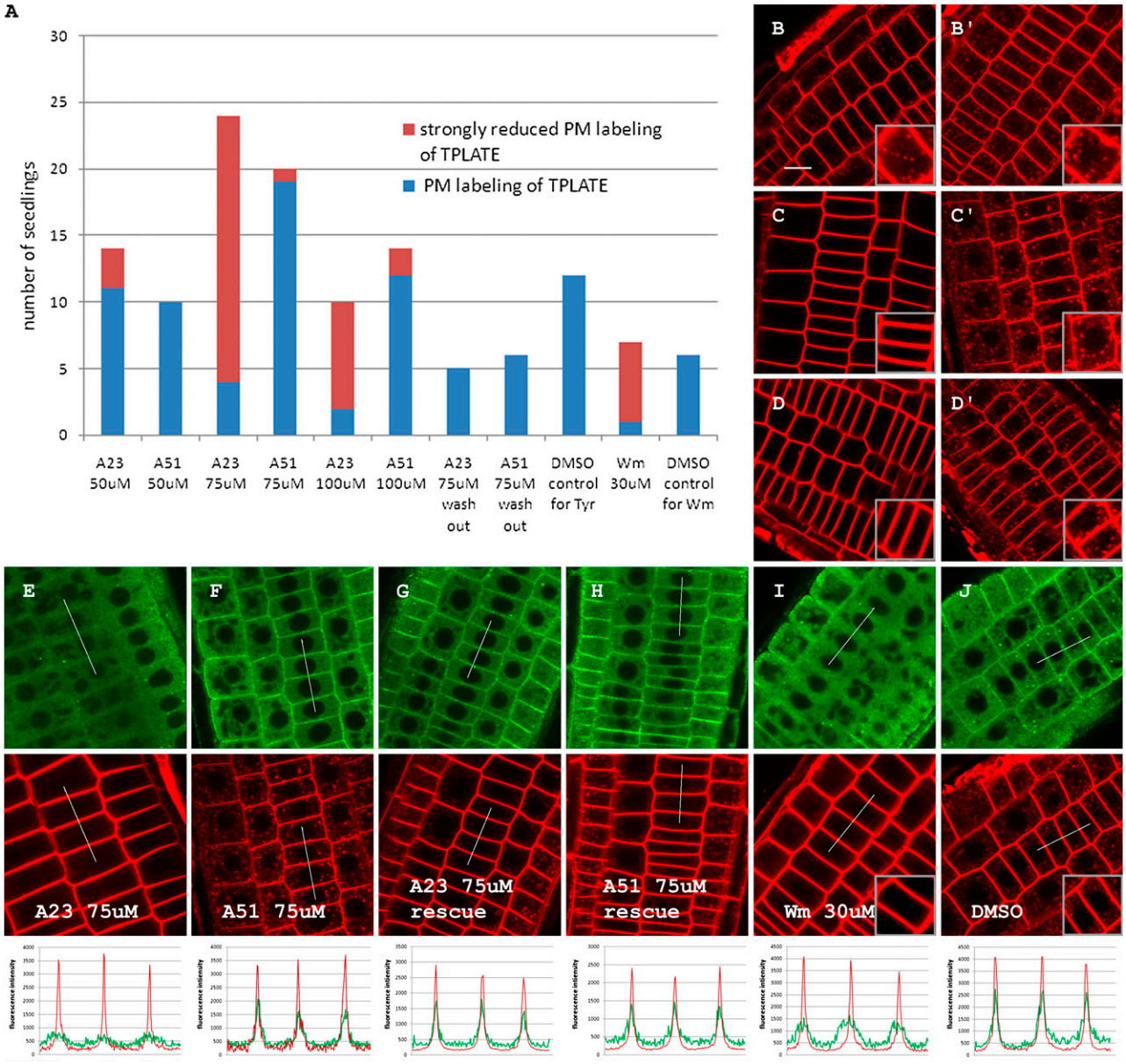

Fig. S5. Tyrphostin and Wortmannin affect PM recruitment of TPLATE. (*A*) Overview of PM recruitment of genomic TPLATE-GFP upon Tyrphostin and Wortmannin treatment in *Arabidopsis* root cells. PM recruitment of TPLATE is specifically affected by Tyrphostin A23 (75 and 100 μM) and Wortmannin (30 μM) treatment. (*B–D*) Representative images of Tyrphostin-treated and FM4-64–stained root cells. Seedlings were treated with Tyrphostin A23 (50 μM, *B*; 75 μM, *C*; and 100 μM, *D*) or Tyrphostin A51 (50 μM, *B′*; 75 μM, *C′*; and 100 μM, *D′*) for 30 min followed by FM4-64 (4 μM) staining in the presence of the drug. Addition of 75 or 100 μM Tyrphostin A23 strongly inhibited FM uptake, in contrast to Tyrphostin A51 treatment. *Insets* represent blowups with increased contrast to visualize uptake of the dye. (*E* and *F*) Representative images of seedlings expressing genomic TPLATE-GFP treated with 75 μM Tyrphostin A23 and A51, showing specific reduction in PM recruitment of TPLATE following Tyrphostin A23 treatment. (*G* and *H*) Wash-out of Tyrphostin A23-treated seedlings restores FM4-64 uptake and PM recruitment of TPLATE-GFP to levels comparable to Tyrphostin A51-treated seedlings. (*I*) Wortmannin (30 μM, 1 h) treatment also inhibited FM4-64 uptake (*Inset*) and abolished PM recruitment of TPLATE-GFP. (*J*) Representative control image of DMSO-treated seedlings showing PM recruitment of TPLATE-GFP and FM4-64 uptake (*Inset*). Fluorescence intensity plots (TPLATE in green and FM4-64 in red) along the white lines in *E–J* further clarify the absence/presence of TPLATE at the PM caused by the respective treatments. All images were taken with identical confocal settings (Scale bar: 10 μm.)

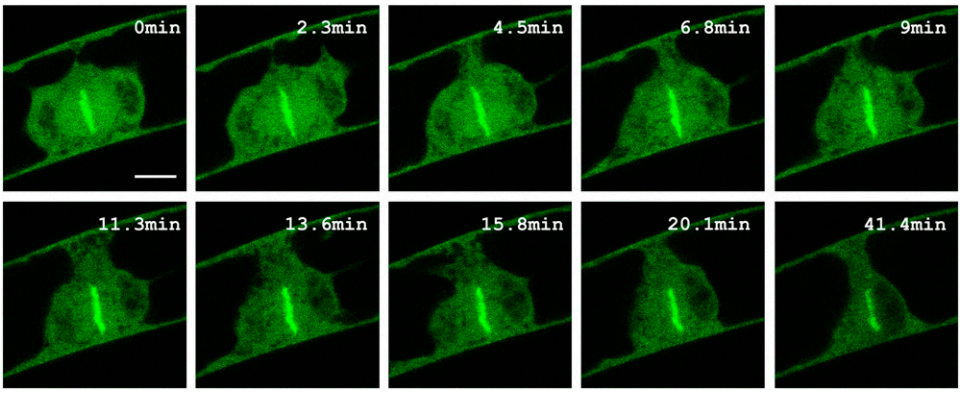

Fig. S6. Division zone association of TPLATE requires phragmoplast expansion. Time-lapse series of a TPLATE-GFP–expressing BY-2 cell treated with 6 μM propyzamide after the onset of cell plate formation. Depolymerization of the phragmoplast microtubules stops cell plate expansion without affecting TPLATE-GFP association with the formed cell plate. Division zone labeling of TPLATE-GFP does not occur, and the cell plate eventually disintegrates. (Scale bar: 10 μm).

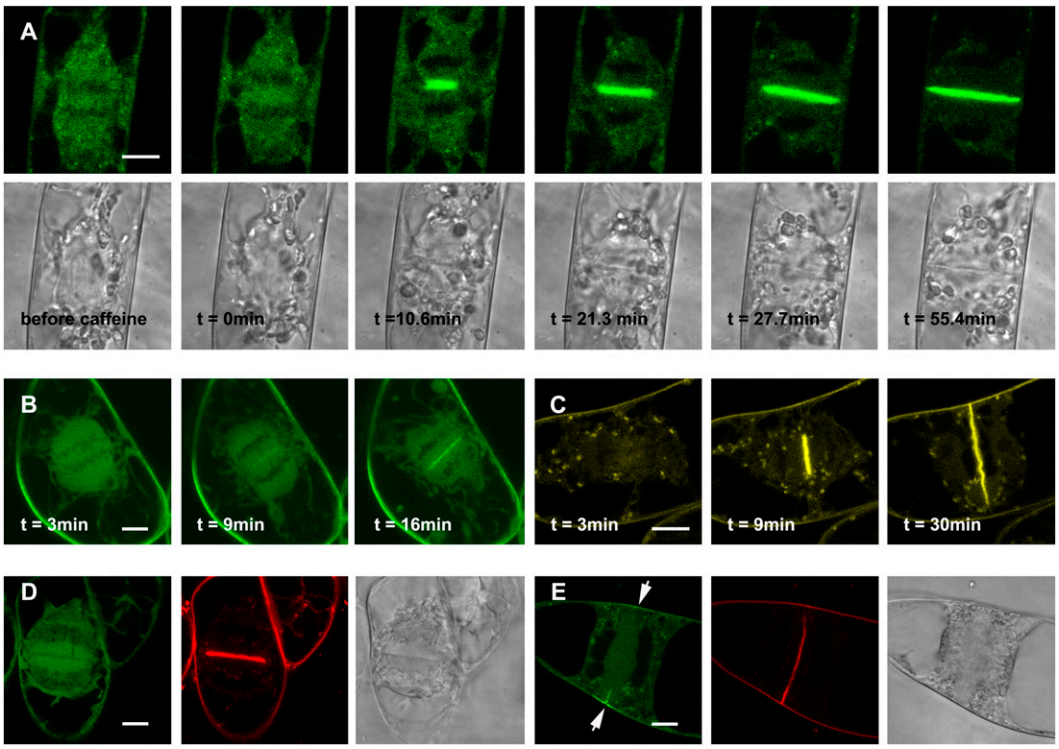

Fig. S7. Caffeine does not abolish cell plate formation in BY-2. (*A*) Anaphase BY-2 cell-expressing FH5-GFP treated with 5 mM caffeine and followed throughout cytokinesis. Cell plate localization of FH-5-GFP is not affected by the drug treatment. (*B* and *C*) Caffeine-treated GFP-KCA1 and mVENUS-PH_{FAPP1} expressing dividing BY-2 cells in the presence of 5 mM caffeine. KCA1 and PH_{FAPP1} targeting is not affected by caffeine treatment. (*D* and *E*) TPLATE-GFP expressing dividing BY-2 cells stained with FM4-64 and treated with caffeine and imaged during early cytokinesis (*D*) and during cell plate anchoring (*E*). TPLATE-GFP is absent from the central cell plate and specifically associates with the plasma membrane at the CDZ (arrows) during anchoring. FM4-64 trafficking to the cell plate is not affected by the caffeine treatment. (Scale bars: 10 μm.)

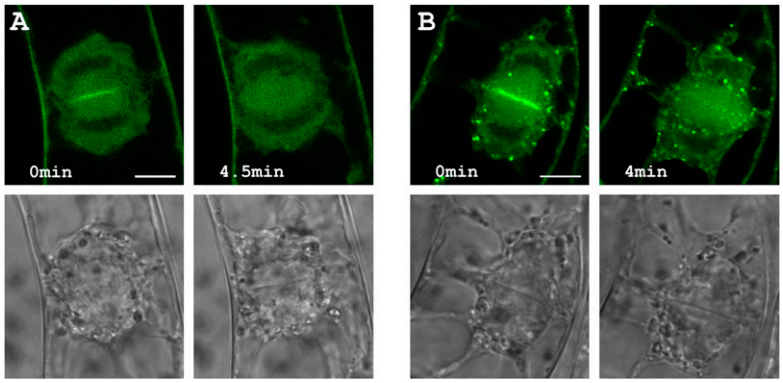

Fig. S8. Caffeine causes rapid delocalization of TPLATE-GFP and CLC2-GFP from the central cell plate. Time-lapse frames of dividing BY-2 cells expressing TPLATE-GFP (*A*) and CLC2-GFP (*B*) treated with 5 mM caffeine during early cell plate formation. Cell plate labeling is lost within minutes after the addition of the drug. The punctate endomembrane localization of CLC2-GFP is not affected by the caffeine treatment, in contrast to the cell plate recruitment of CLC2. (Scale bars: 10 μm.)

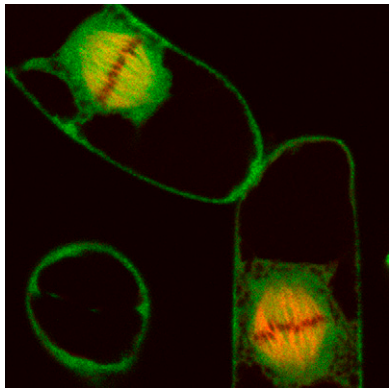

Movie S1. Time lapse series of dividing BY-2 cells expressing TPLATE-GFP and RFP-TUA2 and showing cell plate and CDZ accumulation of TPLATE-GFP. Time = 3 min between frames.

Movie S1

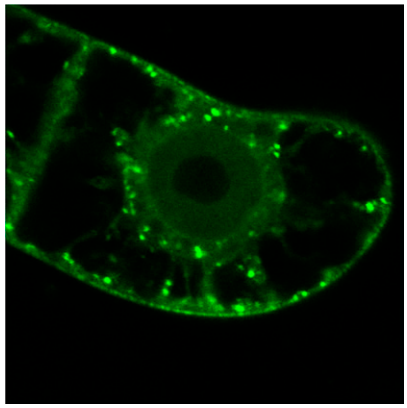

Movie S2. Time lapse series of dividing BY-2 cells expressing CLC2-GFP and showing accumulation of CLC2 at the cell plate and the CDZ during anchoring. Time = 4 min between frames.

Movie S2

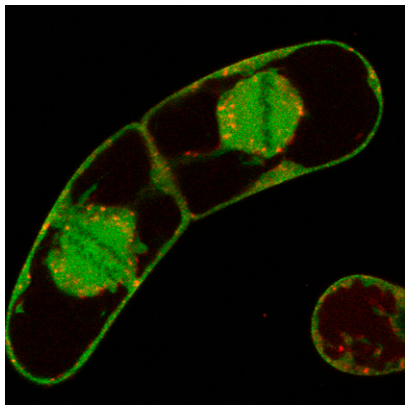

Movie S3. Time lapse series of dividing BY-2 cells expressing TPLATE-GFP and CLC2-mCHERRY and showing colocalization of both proteins at the cell plate and the CDZ during anchoring. This movie was used to create Fig. S2. Time = 4 min between frames.

Movie S3